



Received 23 June 2022

Accepted 30 July 2022

Edited by D. Chopra, Indian Institute of Science
Education and Research Bhopal, India**Keywords:** ethyl 1-(3-tosylquinolin-4-yl)piperidine-4-carboxylate; antibacterial properties; molecular and crystal structure; Hirshfeld surface analysis; pairwise interaction energy; molecular docking.**CCDC reference:** 2193735**Supporting information:** this article has supporting information at journals.iucr.org/e

Synthesis, X-ray diffraction study, analysis of intermolecular interactions and molecular docking of ethyl 1-(3-tosylquinolin-4-yl)piperidine-4-carboxylate

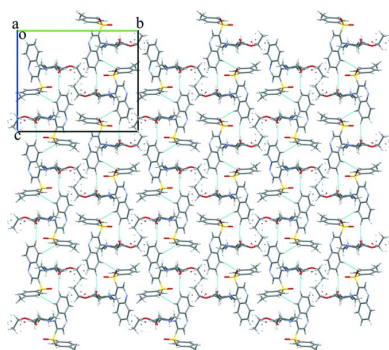
Yevhenii Vaksler,^{a*} Halyna V. Hryhoriv,^b Sergiy M. Kovalenko,^c Lina O. Perekhoda^b and Victoriya A. Georgiyants^b^aSSI Institute for Single Crystals, National Academy of Sciences of Ukraine, 60 Nauky Ave, Kharkov 61001, Ukraine, ^bThe National University of Pharmacy, 53 Pushkinska St., Kharkiv 61002, Ukraine, and ^cV. N. Karazin Kharkiv National University, 4 Svobody Sq., Kharkiv 61077, Ukraine. *Correspondence e-mail: vaksler@gmail.com

The title compound, C₂₄H₂₆N₂O₄S, can be obtained *via* two synthetic routes. According to our investigations, the most suitable way is by the reaction of ethyl 2-bromoacetate with sodium tosylsulfinate in dry DMF. It was crystallized from methanol into the monoclinic *P*2₁/*n* space group with a single molecule in the asymmetric unit. Hirshfeld surface analysis was performed to define the hydrogen bonds and analysis of the two-dimensional fingerprint plots was used to distinguish the different types of interactions. Two very weak non-classical C—H···O hydrogen bonds were found and the contributions of short contacts to the Hirshfeld surface were determined. Molecules form an isotropic network of intermolecular interactions according to an analysis of the pairwise interaction energies. A molecular docking study evaluated the interactions in the title compound with the active centers of macromolecules of bacterial targets (*Staphylococcus aureus* DNA Gyrase PDB ID: 2XCR, *Mycobacterium tuberculosis* topoisomerase II PDB ID: 5BTL, *Streptococcus pneumoniae* topoisomerase IV PDB ID: 4KPF) and revealed high affinity towards them that exceeded the reference antibiotics of the fluoroquinolone group.

1. Chemical context

Quinolone-based compounds have become strikingly conspicuous in recent years. Generally, quinolone derivatives can possess antibacterial, antiparasitic and antiviral (including malaria, hepatitis, HIV, herpes), anticancer and immunosuppressant activities. They can be used in the treatment of obesity, diabetes and neurodegenerative diseases (Horta *et al.*, 2017). Thus, in this work, we decided to broaden the scope of the quinolone scaffolds utilized in our previous works (Bylov *et al.*, 1999; Silin *et al.*, 2004; Savchenko *et al.*, 2007; Hryhoriv *et al.*, 2021) toward a promising new class of arylsulfonylethylquinolin derivatives, namely ethyl 1-(3-tosylquinolin-4-yl)piperidine-4-carboxylate.

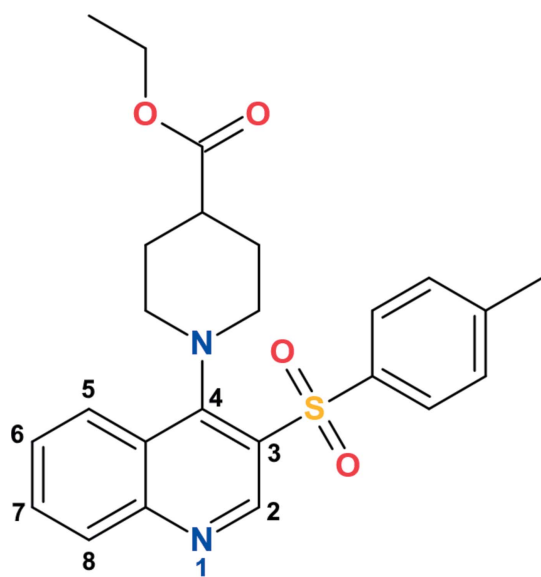
Effective synthetic approaches toward these compounds are versatile. The most notable among them are green chemistry methods and microwave-assisted synthesis (Dhiman *et al.*, 2019; Atechian *et al.* 2007). However, to date, very few data are available for arylsulfonylethylquinolins. Kang *et al.* (2016) described a straightforward and mild one-pot method to synthesize 3-(phenylsulfonyl)-2,3-dihydro-4(1*H*)quinolinones *via* a Cu-catalyzed aza-Michael addition/base-mediated cyclization reaction. Other researchers (Ivachtchenko *et al.*



OPEN ACCESS

Published under a CC BY 4.0 licence

2012*a,b*) have reported new 3-(phenylsulfonyl)quinoline derivatives as serotonin 5-HT receptor antagonists, performed molecular docking studies, and proposed them for preventing and treating central nervous system (CNS) diseases such as psychiatric disorders, schizophrenia, anxiety disorders, and obesity. The preparation method for 3-methanesulfonylquinolines such as GABA-B enhancers was patented by Malherbe *et al.* (2006). *In vivo* investigations of 4-amino-3-arylsulfoquinolin derivatives as metabotropic glutamate 5(mGlu) receptor negative allosteric modulators have shown efficacy for treating anxiety and depression (Galambos *et al.*, 2017).



In the present paper, we study an optimal synthetic route for ethyl 1-(3-tosylquinolin-4-yl)piperidine-4-carboxylate and report its molecular and crystal structures as well as potential biological properties.

2. Structural commentary

The asymmetric unit contains one molecule of ethyl 1-(3-tosylquinolin-4-yl)piperidine-4-carboxylate (Fig. 1). The presence of two bulky substituents in vicinal positions at the pyridine ring results in a rotation of the piperidine ring with respect to the bicyclic fragment [the dihedral angle between their mean planes is $76.83(13)^\circ$]. The piperidine ring adopts a chair conformation with puckering parameters (Zefirov *et al.*, 1990) $S = 1.16(1)$, $\Theta = 0.6(1)^\circ$, $\Psi = 66.2(12)^\circ$. The atoms N2 and C19 deviate from the mean plane of the other ring atoms by $-0.640(2)$ and $0.675(3)$ Å, respectively. The atom N2 has a pyramidal configuration with a bond-angle sum of 345.4° . The ethyl ester group is located in an equatorial position with respect to the piperidine ring [the $C17-C18-C19-C22$ torsion angle is $179.8(2)^\circ$]. It is disordered over the two positions (*A* and *B*) due to rotation around the $C19-C22$ bond with an occupancy ratio of 0.562(12):0.438(12). The ethyl group is almost orthogonal to the carboxylic fragment in conformer *A* and is located in the intermediate position

Table 1
Hydrogen-bond geometry (Å, °).

$D-H\cdots A$	$D-H$	$H\cdots A$	$D\cdots A$	$D-H\cdots A$
$C4-H4\cdots O3A^i$	0.93	2.52	3.421 (16)	163
$C5-H5\cdots O2^{ii}$	0.93	2.58	3.415 (4)	149

Symmetry codes: (i) $x - \frac{1}{2}, -y + \frac{3}{2}, z + \frac{1}{2}$; (ii) $x + \frac{1}{2}, -y + \frac{3}{2}, z + \frac{1}{2}$.

between *ac* and *ap* in conformer *B* [the $C22-O4-C23-C24$ torsion angle is $-98.1(14)$ and $150(2)^\circ$ in conformers *A* and *B*, respectively]. The tolyl substituent is located in a *sc* position relative to the endocyclic $C7-C8$ bond [$C7-C8-S1-C10 = -71.5(3)^\circ$] and rotated about the $C8-S1$ bond [$C8-S1-C10-C11 = 124.9(2)^\circ$].

3. Supramolecular features

Regarding the van der Waals radii proposed in Bondi (1964) for all atoms except for the hydrogens (Rowland & Taylor, 1996), the analysis of intermolecular interactions revealed two very weak non-classical hydrogen bonds, $C4-H4\cdots O3A$ and $C5-H5\cdots O2$ (Table 1). The first is formed by an oxygen atom of the carboxylic group and a hydrogen atom of the benzene ring (Fig. 2*a*). An oxygen atom of the sulfonyl group is involved in the second hydrogen bond, similarly with a hydrogen atom of the benzene ring (Fig. 2*b*). Connected with the initial molecule by the symmetry operations $x - \frac{1}{2}, -y + \frac{3}{2}, z + \frac{1}{2}$ and $x + \frac{1}{2}, -y + \frac{3}{2}, z + \frac{1}{2}$, these hydrogen bonds are affected by both twofold screw axes $\langle 010 \rangle$ and glide plane family $\{010\}$. On their own, these hydrogen bonds form the chains in the $[10\bar{1}]$ and $[101]$ directions, respectively.

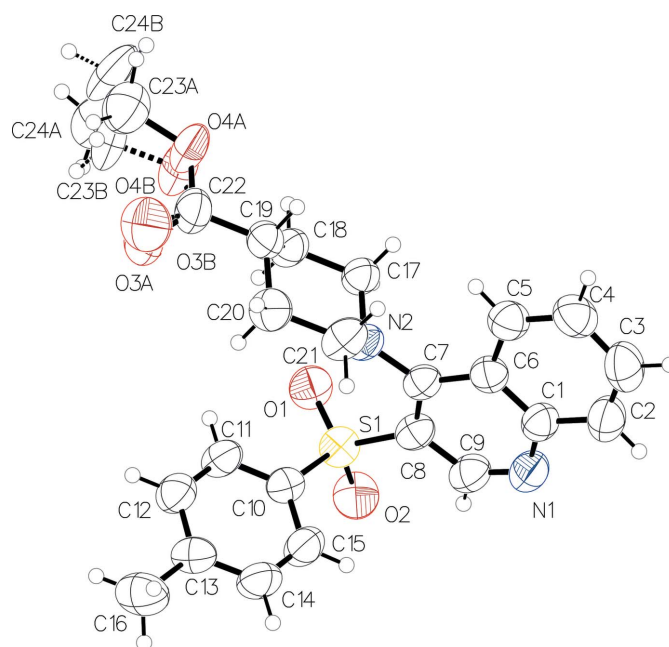


Figure 1
Molecular structure of the title compound. Displacement ellipsoids are shown at the 50% probability level.

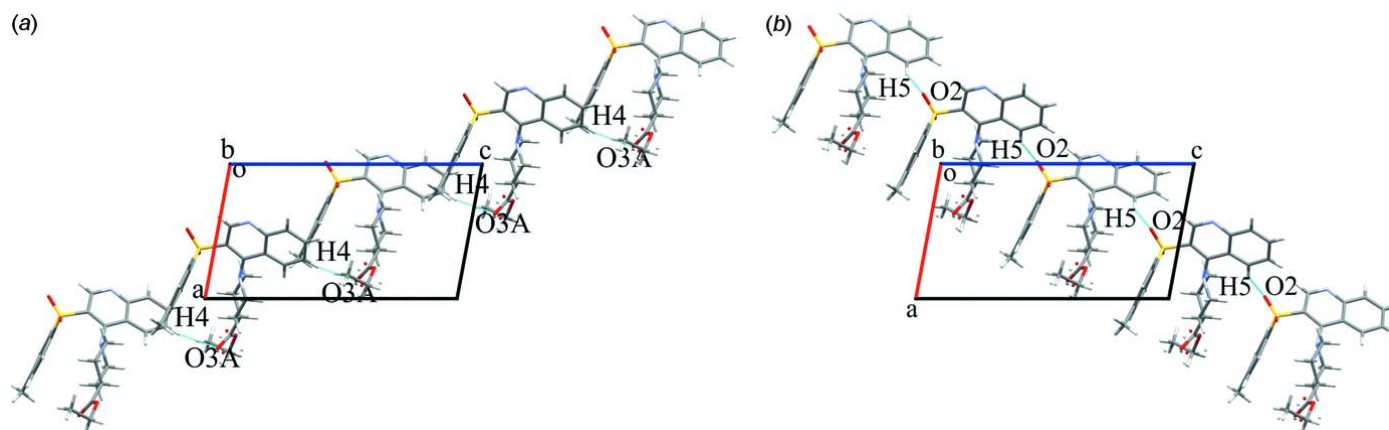


Figure 2
Crystal packing of the chains built with the hydrogen bonds C4–H4···O3A (a) and C5–H5···O2 (b) in cyan. Projection in the [010] direction.

4. Hirshfeld surface analysis

The complementation of the Hirshfeld surface, *i.e.* the surface splitting the regions of crystal into molecular domains within the ratio of promolecular to procrystal electronic density, with geometric parameters, especially the normalized contact distance (d_{norm}), implemented in *CrystalExplorer17* (Spackman *et al.*, 2021) allowed us to distinguish the intermolecular interactions in a more thorough way. The standard ‘high’ surface resolution was used. Two regions with d_{norm} significantly lower than the van der Waals contact length (in red) emerge on the surface (Fig. 3a). Both of them concern the C4–H4···O3A hydrogen bond and show it to be the sole directed interaction in the crystal. The chains built up by these hydrogen bonds are parallel to the $[\bar{1}01]$ direction. However, they cannot be considered as a structural motif because the aforementioned hydrogen bonds are very weak, exist solely for conformer *A* and one of them was not revealed for conformer *B*. At the same time, the short contact C24B···O1 appears just for conformer *B* (Fig. 3b). Differences in the distribution of d_{norm} for the two conformers and so the short

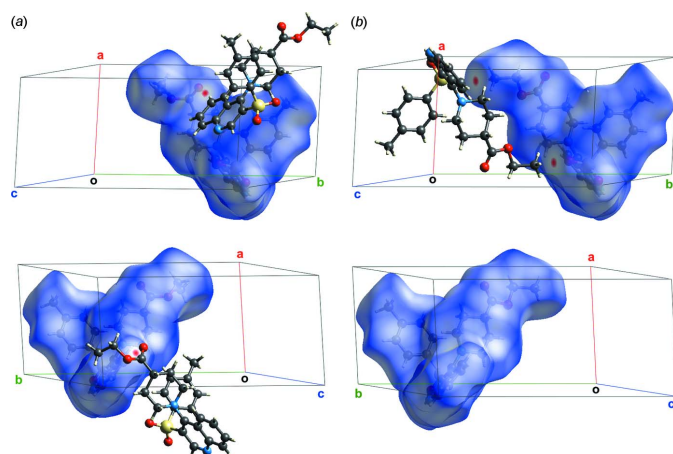


Figure 3
Distribution of the value d_{norm} onto the Hirshfeld surfaces of the conformers *A* (a) and *B* (b).

contacts and hydrogen bonds can be easily be seen from the two projections (top and bottom) shown in Fig. 3.

In addition to the Hirshfeld surface analysis, the 2D fingerprint plots were computed for ethyl 1-(3-tosylquinolin-4-yl)piperidine-4-carboxylate. The contributions of the three types of intermolecular contacts get to areas with the values of the internal and external distances (d_i and d_e) below the van der Waals radii of the corresponding atoms (Fig. 4). These contributions belong to the short O···H, C···H and H···H contacts. They are 20.2% and 19.9% of the Hirshfeld surface area for H···O/O···H for the disorder components *A* and *B*, respectively, 16.7% and 17.7%, respectively, for C···H/H···C and 54.3% for H···H. The differences for the disordered positions *A* and *B* can be explained by the rearrangement of the interactions network described above.

5. Analysis of the pairwise interaction energies

The strength of the non-classical C–H···O hydrogen bonds is often underestimated, as mentioned in Sutor (1962) and Desiraju (1996, 2005). Thus, to extend the knowledge of the supramolecular structure of the title compound and to prove the small contribution of these interactions to the structure, analysis of the pairwise interaction energies was performed as proposed by Konovalova *et al.* (2010) and Shishkin *et al.* (2012). The procedure was implied in a very similar way to the one described in detail in Vaksler *et al.* (2021). The single

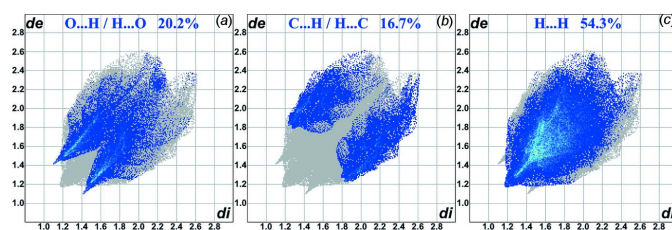


Figure 4
Contributions of the O···H/H···O (a), C···H/H···C (b) and H···H (c) contacts to the fingerprint plots built using the Hirshfeld surfaces of conformer *A*.

molecule was considered as a building unit. The interactions in the molecular pairs containing the aforementioned hydrogen bonds are -7.4 and -10.5 kcal mol $^{-1}$ for conformer *A* and -3.2 and -11.7 kcal mol $^{-1}$ for conformer *B* (data given for the C24B \cdots O1 short contact and the C5–H5 \cdots O2 hydrogen bond). These values are comparable to those for the non-directed interactions in other pairs of neighboring molecules. In addition to this, the interaction energy decomposition was performed using an ‘accurate’ energy model in *Crystal-Explorer17* for the molecular pairs with C–H \cdots O hydrogen bonds. It showed that the sum of electrostatic and polarization components is rather low in comparison with the dispersion and repulsion terms (-1.0 versus -7.5 and 2.6 kcal mol $^{-1}$ for the C4–H4 \cdots O3A hydrogen bond, -4.6 versus -9.7 and 4.2 kcal mol $^{-1}$ for C5–H5 \cdots O2) implying minimal contributions of hydrogen bonds in general bonding. Despite the apparent layering (Fig. 5a) parallel to the (010) plane, the energetic structure of the title compound can be considered isotropic, which can easily be seen from the energy vector diagrams (Fig. 5b). The total energy of interaction between a basic molecule and its first coordination sphere is -95.8 and -95.5 kcal mol $^{-1}$ for conformers *A* and *B*, respectively.

6. Database survey

A search of the Cambridge Structural Database [Version 5.42, update of November 2020; Groom *et al.*, 2016] shows no similarities between the title compound and 4-(piperidin-1-yl)-3-sulfone-quinoline derivatives.

7. Molecular docking

A molecular docking study was performed in order to estimate the application efficiency of ethyl 1-(3-tosylquinolin-4-yl)pi-

Table 2

The values of affinity DG, free binding energy, and binding coefficients for the best conformational positions of the title compound in combination with biotargets (PDB ID: 2XCR, 5BTL, 4KPF). Values are also given for reference compounds.

Molecule	Affinity DG (kcal mol $^{-1}$)	E_{Doe} (kcal mol $^{-1}$)	K_i (μM)
PDB ID: 2XCR			
Title compound	–7.5	–5.62	76.15
Ciprofloxacin	–7.2	–5.10	183.79
Norfloxacin	–7.2	–4.30	708.28
PDB ID: 5BTL			
Title compound	–8.2	–5.64	73.02
Ciprofloxacin	–7.5	–5.51	91.69
Norfloxacin	–7.8	–5.25	142.92
PDB ID: 4KPF			
Title compound	–8.1	–6.13	31.90
Ciprofloxacin	–7.4	–5.38	113.52
Norfloxacin	–7.4	–4.78	315.73

peridine-4-carboxylate in terms of medicinal chemistry as antimicrobials. For receptor-oriented flexible docking, the *Autodock 4.2* software package (Morris *et al.*, 2009) was used. Ligands were prepared using the *MGL Tools 1.5.6* (Sanner, 1999) and optimized within the *Avogadro* (Hanwell *et al.*, 2012) (United Force Field with the steepest descent algorithm). The biotargets were chosen on the basis of structural similarity between the title compound and known antibacterial agents from the group of fluoroquinolones. The active centers of macromolecules of bacterial targets [*Staphylococcus aureus* DNA Gyrase PDB ID: 2XCR (Bax *et al.*, 2010); *Mycobacterium tuberculosis* topoisomerase II PDB ID: 5BTL (Blower *et al.*, 2016); *Streptococcus pneumoniae* topoisomerase IV PDB ID: 4KPF (Laponogov *et al.*, 2016)] from the Protein Data Bank (PDB) were used for docking.

The receptor maps were made with *MGL Tools* and *AutoGrid* (Sanner, 1999). The docking parameters were defined closely to the ones mentioned in Syngiun *et al.* (2016;

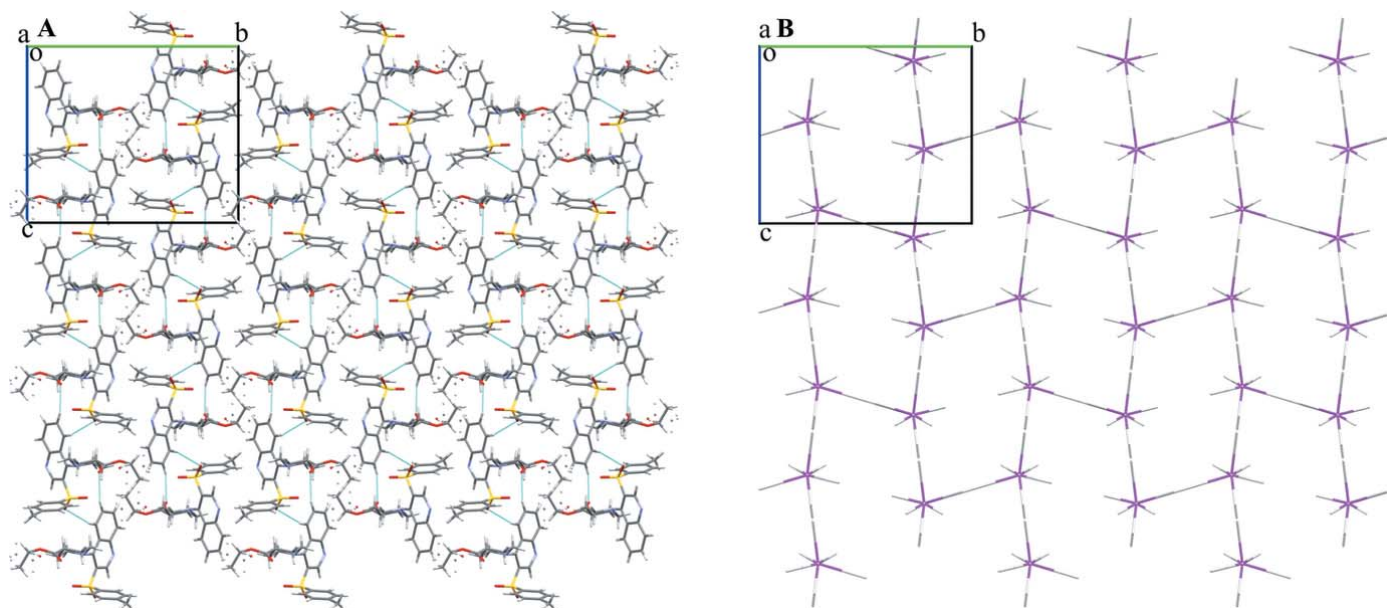


Figure 5
Crystal packing of the molecules (*a*) and energy vector diagrams (*b*). Projection in the [100] direction.

see supporting information). These parameters were chosen to bring the formation of a complex between the tested molecule and the receptor as close as possible to the conditions that exist in biological systems.

Inhibitory activity against bacterial targets can be realized by the formation of their complexes with ligands [as ethyl 1-(3-tosylquinolin-4-yl)piperidine-4-carboxylate]. In turn, the stability of complexes can be estimated from the strength of the intermolecular interactions. The scoring function indicating the enthalpy contribution to the value of the free binding energy (affinity DG), the values of the free binding energy and binding constants [E_{Doc} (kcal mol⁻¹) and K_i (μM)] are represented for the most profitable conformation positions (Table 2). All the parameters show that the title compound is superior to the reference medicines of the same type.

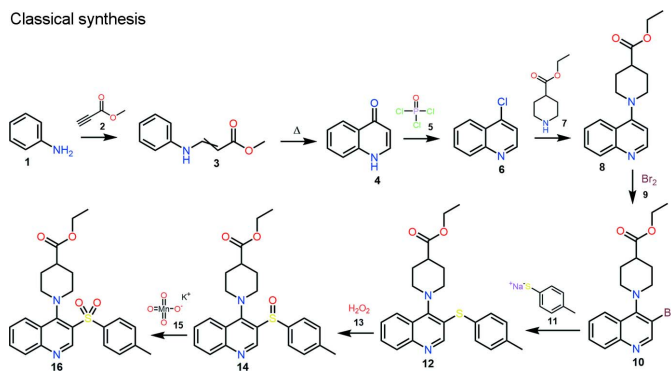
8. Synthesis and crystallization

The starting compounds were obtained from commercial sources and were used without further purification.

Two ways were proposed for the synthesis of ethyl 1-(3-tosylquinolin-4-yl)piperidine-4-carboxylate: the classical one and an alternative one with a lower number of steps and higher yield of the final product:

Classical synthesis. In the first stage, the addition of methyl propiolate **2** to aniline **1** produces labile *cis-trans* mixtures of enamine **3**. Thermal cyclization of enamine **3** provides a synthesis of 4(1*H*)-quinolone **4** (Gray *et al.*, 1951).

Classical synthesis

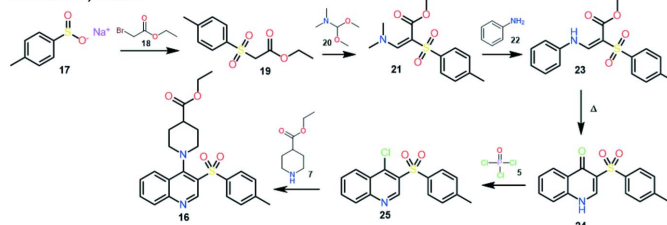


Conversion of 4-hydroxyquinoline **4** to 4-chloroquinoline **6** can be carried out by a known halogenation method with POCl_3 **5**, or other suitable reagents (*e.g.* SOCl_2 , PCl_5 , POBr_3 , PBr_3). The obtained 4-chloroquinoline **6** can be converted to 4-aminoquinoline derivative **8** by an aromatic nucleophilic substitution reaction with secondary amine **7**. Standard bromination of quinoline **8** gives the product **10**. 4-Amino-3-bromoquinoline **10** can be substituted by the sodium salt of thiophenol **11** to provide compound **12**. Oxidation of 4-amino-3-arylsulfanylquinoline **12** can be accomplished by known methods, preferably in a suitable acid (*e.g.* acetic acid) at 273–278 K with potassium permanganate **15** to give 4-amino-3-arylsulfinylquinolines **14** or with aqueous hydrogen peroxide **13** in a suitable acid (*e.g.* acetic acid or trifluoroacetic acid). To obtain the title compound **16**, further oxidation of compound

14 is required. The reaction can be carried out by known methods, preferably in a suitable acid (*e.g.* acetic acid) at 273–278 K with potassium permanganate **15** (Keserü *et al.*, 2007). The yield of the title compound is 46.0%.

Alternative synthesis. Ethyl 2-tosylacetate **19** is obtained by the reaction of ethyl 2-bromoacetate **18** with sodium tosylsulfinate **17** in dry DMF. Compound **21** can be obtained by the condensation reaction of compound **19** with *N,N*-dimethylformamide dimethylacetal **20** without using a solvent or in a minimum amount of dioxane. Compound **21**, upon reaction with aniline **22** in isopropanol/AcOH medium, produces an *E/Z* isomer mixture of enamine **23**, which is converted to 3-tosylquinoline-4-(1*H*)-one **24** by thermal cyclization in diphenyl ether. Chlorination of compound **24** is carried out according to a known method with phosphorus oxychloride **5**. The final product **16** is obtained by the reaction of aromatic nucleophilic substitution of 4-chloro-3-tosylquinoline **25** with ethyl piperidine-4-carboxylate **7** in a dry DMF medium using a base (triethylamine, DBU), or excess of secondary amine (Keserü *et al.*, 2007). The yield of the title compound is 73.6%. Recrystallization by slow evaporation of a solution in acetonitrile produced block-like colorless crystals suitable for X-ray diffraction analysis. The advantages of this synthesis make it seem preferable to the common one.

Alternative synthesis



9. NMR characterization

The NMR spectra were recorded on a Varian MR-400 spectrometer with standard pulse sequences operating at 400 MHz for ¹H NMR, 101 MHz for ¹³C NMR. For the NMR spectra, DMSO-*d*₆ was used as a solvent. Chemical shift values are referenced to residual protons (δ 2.49 ppm) and carbons (δ 39.6 ppm) of the solvent as an internal standard. LC/MS spectra were recorded on a ELSD Alltech 3300 liquid chromatograph equipped with a UV detector (λ_{max} 254 nm), API-150EX mass-spectrometer using a Zorbax SB-C18 column, Phenomenex (100 × 4 mm) Rapid Resolution HT Cartridge 4.6 × 30mm, 1.8-Micron. Elution started with an 0.1 M solution of HCOOH in water and ended with an 0.1 M solution of HCOOH in acetonitrile using a linear gradient at a flow rate of 0.15 ml min⁻¹ and an analysis cycle time of 25 min.

Characteristics of the title molecule:

¹H NMR (400 MHz, DMSO-*d*₆) δ 9.37 (s, 1H), 8.28 (d, J = 8.6 Hz, 1H), 8.17 (d, J = 8.4 Hz, 1H), 7.93 (t, J = 7.7 Hz, 1H), 7.72 (t, J = 8.0 Hz, 3H), 7.39 (d, J = 8.0 Hz, 2H), 4.10 (q, J = 7.1 Hz, 2H), 3.37 (d, J = 19.2 Hz, 1H), 3.31–3.27 (m, 1H), 2.92 (d, J = 11.2 Hz, 2H), 2.55 (d, J = 9.2 Hz, 1H), 2.38 (s, 3H), 1.64 (dd, J = 13.2, 3.8 Hz, 2H), 1.41–1.36 (m, 1H), 1.35 (s, 1H), 1.22 (t, J = 7.1 Hz, 3H).

Table 3

Experimental details.

Crystal data	
Chemical formula	C ₂₄ H ₂₆ N ₂ O ₄ S
<i>M_r</i>	438.53
Crystal system, space group	Monoclinic, <i>P</i> ₂ ₁ / <i>n</i>
Temperature (K)	298
<i>a</i> , <i>b</i> , <i>c</i> (Å)	8.2608 (3), 17.9433 (7), 15.2470 (7)
β (°)	100.626 (4)
<i>V</i> (Å ³)	2221.25 (16)
<i>Z</i>	4
Radiation type	Mo <i>K</i> α
μ (mm ⁻¹)	0.18
Crystal size (mm)	0.3 × 0.2 × 0.1
Data collection	
Diffractometer	Xcalibur, Sapphire3
Absorption correction	Multi-scan (<i>CrysAlis PRO</i> ; Rigaku OD, 2018)
<i>T</i> _{min} , <i>T</i> _{max}	0.400, 1.000
No. of measured, independent and observed [<i>I</i> > 2 σ (<i>I</i>)] reflections	22680, 6477, 3049
<i>R</i> _{int}	0.104
(<i>sin</i> θ / λ) _{max} (Å ⁻¹)	0.703
Refinement	
<i>R</i> [<i>F</i> ² > 2 σ (<i>F</i> ²)], <i>wR</i> (<i>F</i> ²), <i>S</i>	0.077, 0.253, 1.04
No. of reflections	6477
No. of parameters	321
No. of restraints	9
H-atom treatment	H-atom parameters constrained
$\Delta\rho_{\text{max}}$, $\Delta\rho_{\text{min}}$ (e Å ⁻³)	0.33, -0.52

Computer programs: *CrysAlis PRO* (Rigaku OD, 2018), *SHELXT2014/5* (Sheldrick, 2015a), *SHELXL2017/1* (Sheldrick, 2015b) and *OLEX2* (Dolomanov et al., 2009).

¹³C NMR (101 MHz, DMSO-*d*₆) δ 174.17, 158.14, 151.56, 149.44, 143.64, 139.23, 132.37, 130.31, 129.66, 127.43, 126.19, 125.86, 59.85, 50.56, 27.26, 21.02, 14.11.

10. Refinement

Crystal data, data collection and structure refinement details are summarized in Table 3. All hydrogen atoms were positioned geometrically (C–H = 0.93–0.97 Å) and refined using a riding model with $U_{\text{iso}}(\text{H}) = nU_{\text{eq}}$ of the carrier atom ($n = 1.5$ for methyl groups and $n = 1.2$ for other hydrogen atoms). During the refinement the distances between the atoms of the disordered part were restrained to the following values: 1.497 Å for the bond C19–C22, 1.196 Å for O3–C22, 1.336 Å for O4–C22, 1.452 Å for O4–C23 and 1.513 Å for C23–C24 according to the mean values in Dunitz & Bürgi (1994). The estimated standard deviation was set at 0.005 Å for all the bonds.

Funding information

Funding for this research was provided by: Ministry of Health of Ukraine (grant No. 0121U109239).

References

Atechian, S., Nock, N., Norcross, R. D., Ratni, H., Thomas, A. W., Verron, J. & Masciadri, R. (2007). *Tetrahedron*, **63**, 2811–2823.
 Bax, B. D., Chan, P. F., Eggleston, D. S., Fosberry, A., Gentry, D. R., Gorrec, F., Giordano, I., Hann, M. M., Hennessy, A., Hibbs, M.,

Huang, J., Jones, E., Jones, J., Brown, K. K., Lewis, C. J., May, E. W., Saunders, M. R., Singh, O., Spitzfaden, C. E., Shen, C., Shillings, A., Theobald, A. J., Wohlkonig, A., Pearson, N. D. & Gwynn, M. N. (2010). *Nature*, **466**, 935–940.
 Blower, T. R., Williamson, B. H., Kerns, R. J. & Berger, J. M. (2016). *PNAS* **113**, 7, 1706–1713.
 Bondi, A. (1964). *J. Phys. Chem.* **68**, 3, 441–451.
 Bylov, I. E., Bilokin, Y. V. & Kovalenko, S. M. (1999). *Heterocycl. Comm.* **5**, 3, 281–284.
 Desiraju, G. R. (1996). *Acc. Chem. Res.* **29**, 441–449.
 Desiraju, G. R. (2005). *ChemComm*, **24**, 2995–3001.
 Dhiman, P., Arora, N., Thanikachalam, P. V. & Monga, V. (2019). *Bioorg. Chem.* **92**, 103291.
 Dolomanov, O. V., Bourhis, L. J., Gildea, R. J., Howard, J. A. K. & Puschmann, H. (2009). *J. Appl. Cryst.* **42**, 339–341.
 Dunitz, J. D. & Bürgi, H.-B. (1994). *Structure correlation*, pp. 767–784. Weinheim: VCH.
 Galambos, J., Bielik, A., Wágner, G., Domány, G., Kóti, J., Béni, Z., Szigetvári, Á., Sánta, Z., Orgován, Z., Bobok, A., Kiss, B., Mikó-Bakk, M. L., Vastag, M., Sággy, K., Krasavin, M., Gál, K., Greiner, I., Szombathelyi, Z. & Keserű, G. M. (2017). *Eur. J. Med. Chem.* **133**, 240–254.
 Gray, F. W., Mosher, H. S., Whitmole, F. C. & Oakwood, T. S. (1951). *J. Am. Chem. Soc.* **73**, 8, 3577–3578.
 Groom, C. R., Bruno, I. J., Lightfoot, M. P. & Ward, S. C. (2016). *Acta Cryst. B72*, 171–179.
 Hanwell, M. D., Curtis, D. E., Lonie, D. C., Vandermeersch, T., Zurek, E. & Hutchison, G. R. (2012). *J. Cheminform.* **4**, 17.
 Horta, P., Secrieru, A., Coninckx, A. & Cristiano, M. L. S. (2017). *OMCII*, **4**, 91–93.
 Hryhoriv, H., Mariutsa, I., Kovalenko, S., Sidorenko, L., Perekhoda, L., Filimonova, N., Geyderikh, O. & Georgiyants, V. (2021). *ScienceRise Pharm. Sci.* **5**, 33, 4–11.
 Ivachtchenko, A. V., Golovina, E. S., Kadieva, M. G., Kysil, V. M., Mitkin, O. D., Vorobiev, A. A. & Okun, I. (2012a). *Bioorg. Med. Chem. Lett.* **22**, 4273–4280.
 Ivachtchenko, A. V., Mitkin, O. D. & Kadieva, M. G. (2012b). Patent WO/2012/087182.
 Kang, S., Yoon, H. & Lee, Y. (2016). *Chem. Lett.* **45**, 1356–1358.
 Keserű, G., Wéber, C., Bielik, A., Bobok, A. A., Gál, K., Meszlényiné Sipos, M., Molnár, L. & Vastag, M. (2007). Patent WO/2007/072093.
 Konovalova, I. S., Shishkina, S. V., Paponov, B. V. & Shishkin, O. V. (2010). *CrystEngComm*, **12**, 3, 909–916.
 Laponogov, I., Pan, X.-S., Veselkov, D. A., Cirz, R. T., Wagman, A., Moser, H. E., Fisher, L. M. & Sanderson, M. R. (2016). *Open Biol.* **6**, 160157. <https://doi.org/10.1098/rsob.160157>.
 Malherbe, P., Masciadri, R., Norcross, R. D. & Prinssen, E. (2006). Patent WO/2006/128802.
 Morris, G. M., Huey, R., Lindstrom, W., Sanner, M. F., Belew, R. K., Goodsell, D. S. & Olson, A. J. (2009). *J. Comp. Chem.* **30**, 2785–2791.
 Rigaku OD (2018). *CrysAlis PRO*. Rigaku Oxford Diffraction, Yarnton, England.
 Rowland, R. S. & Taylor, R. (1996). *J. Phys. Chem.* **100**, 18, 7384–7391.
 Sanner, M. F. (1999). *J. Mol. Graph. Mod.* **17**, 57–61.
 Savchenko, T. I., Silin, O. V., Kovalenko, S. M., Musatov, V. I., Nikitchenko, V. M. & Ivachtchenko, A. V. (2007). *Synth. Commun.* **37**, 8, 1321–1330.
 Sheldrick, G. M. (2015a). *Acta Cryst. A71*, 3–8.
 Sheldrick, G. M. (2015b). *Acta Cryst. C71*, 3–8.
 Shishkin, O. V., Dyakonov, V. V. & Maleev, A. V. (2012). *CrystEngComm*, **14**, 5, 1795–1804.
 Silin, O. V., Savchenko, T. I., Kovalenko, S. M., Nikitchenko, V. M. & Ivachtchenko, A. V. (2004). *Heterocycles*, **63**, 8, 1883–1890.
 Spackman, P. R., Turner, M. J., McKinnon, J. J., Wolff, S. K., Grimwood, D. J., Jayatilaka, D. & Spackman, M. A. (2021). *J. Appl. Cryst.* **54**, 1006–1011.

- Sutor, D. J. (1962). *Nature*, **195**, 68–69.
- Syniugin, A. R., Ostrynska, O. V., Chekanov, M. O., Volynets, G. P., Starosyla, S. A., Bdzhola, V. G. & Yarmoluk, S. M. (2016). *J. Enzyme Inhib. Med. Chem.* **31**, 160–169.
- Vaksler, Ye. A., Idrissi, A., Urzhuntseva, V. V. & Shishkina, S. V. (2021). *Cryst. Growth Des.* **21**, 4, 2176–2186.
- Zefirov, N. S., Palyulin, V. A. & Dashevskaya, E. E. (1990). *J. Phys. Org. Chem.* **3**, 147–158.

supporting information

Acta Cryst. (2022). E78, 890-896 [https://doi.org/10.1107/S2056989022007691]

Synthesis, X-ray diffraction study, analysis of intermolecular interactions and molecular docking of ethyl 1-(3-tosylquinolin-4-yl)piperidine-4-carboxylate

Yevhenii Vaksler, Halyna V. Hryhoriv, Sergiy M. Kovalenko, Lina O. Perekhoda and Victoriya A. Georgiyants

Computing details

Data collection: *CrysAlis PRO* (Rigaku OD, 2018); cell refinement: *CrysAlis PRO* (Rigaku OD, 2018); data reduction: *CrysAlis PRO* (Rigaku OD, 2018); program(s) used to solve structure: *SHELXT2014/5* (Sheldrick, 2015a); program(s) used to refine structure: *SHELXL2017/1* (Sheldrick, 2015b); molecular graphics: *OLEX2* (Dolomanov *et al.*, 2009); software used to prepare material for publication: *OLEX2* (Dolomanov *et al.*, 2009).

Ethyl 1-[3-(4-methylbenzenesulfonyl)quinolin-4-yl]piperidine-4-carboxylate

Crystal data

$C_{24}H_{26}N_2O_4S$

$M_r = 438.53$

Monoclinic, $P2_1/n$

$a = 8.2608$ (3) Å

$b = 17.9433$ (7) Å

$c = 15.2470$ (7) Å

$\beta = 100.626$ (4)°

$V = 2221.25$ (16) Å³

$Z = 4$

$F(000) = 928$

$D_x = 1.311$ Mg m⁻³

Mo $K\alpha$ radiation, $\lambda = 0.71073$ Å

Cell parameters from 2249 reflections

$\theta = 3.5$ – 22.9 °

$\mu = 0.18$ mm⁻¹

$T = 298$ K

Block, colourless

$0.3 \times 0.2 \times 0.1$ mm

Data collection

Xcalibur, Sapphire3
diffractometer

Radiation source: fine-focus sealed X-ray tube,
Enhance (Mo) X-ray Source

Graphite monochromator

Detector resolution: 16.1827 pixels mm⁻¹

ω scans

Absorption correction: multi-scan
(*CrysAlisPro*; Rigaku OD, 2018)

$T_{\min} = 0.400$, $T_{\max} = 1.000$

22680 measured reflections

6477 independent reflections

3049 reflections with $I > 2\sigma(I)$

$R_{\text{int}} = 0.104$

$\theta_{\max} = 30.0$ °, $\theta_{\min} = 3.0$ °

$h = -11 \rightarrow 11$

$k = -25 \rightarrow 24$

$l = -21 \rightarrow 20$

Refinement

Refinement on F^2

Least-squares matrix: full

$R[F^2 > 2\sigma(F^2)] = 0.077$

$wR(F^2) = 0.253$

$S = 1.04$

6477 reflections

321 parameters

9 restraints

Primary atom site location: structure-invariant
direct methods

Hydrogen site location: inferred from
neighbouring sites

H-atom parameters constrained

$w = 1/[\sigma^2(F_o^2) + (0.106P)^2]$

where $P = (F_o^2 + 2F_c^2)/3$

$(\Delta/\sigma)_{\max} < 0.001$

$$\Delta\rho_{\max} = 0.33 \text{ e } \text{\AA}^{-3}$$

$$\Delta\rho_{\min} = -0.52 \text{ e } \text{\AA}^{-3}$$

Extinction correction: SHELXL-2017/1
(Sheldrick 2015b),
 $F_c^* = kFc[1 + 0.001xFc^2\lambda^3/\sin(2\theta)]^{-1/4}$
Extinction coefficient: 0.0057 (16)

Special details

Geometry. All esds (except the esd in the dihedral angle between two l.s. planes) are estimated using the full covariance matrix. The cell esds are taken into account individually in the estimation of esds in distances, angles and torsion angles; correlations between esds in cell parameters are only used when they are defined by crystal symmetry. An approximate (isotropic) treatment of cell esds is used for estimating esds involving l.s. planes.

Fractional atomic coordinates and isotropic or equivalent isotropic displacement parameters (\AA^2)

	<i>x</i>	<i>y</i>	<i>z</i>	$U_{\text{iso}}^*/U_{\text{eq}}$	Occ. (<1)
S1	0.12710 (8)	0.79643 (4)	0.44018 (5)	0.0610 (3)	
O1	0.1623 (3)	0.71849 (11)	0.44202 (15)	0.0728 (6)	
O2	-0.0150 (2)	0.82165 (14)	0.37816 (14)	0.0790 (6)	
N1	-0.0721 (3)	0.90921 (14)	0.61830 (19)	0.0700 (7)	
N2	0.3448 (3)	0.76877 (12)	0.62148 (16)	0.0557 (6)	
C1	0.0279 (4)	0.89220 (16)	0.6975 (2)	0.0608 (7)	
C2	-0.0099 (4)	0.92616 (19)	0.7745 (2)	0.0765 (9)	
H2	-0.095862	0.960273	0.769311	0.092*	
C3	0.0792 (5)	0.9093 (2)	0.8568 (3)	0.0852 (10)	
H3	0.055013	0.932402	0.907452	0.102*	
C4	0.2055 (5)	0.8577 (2)	0.8645 (2)	0.0811 (10)	
H4	0.262181	0.844427	0.920871	0.097*	
C5	0.2481 (4)	0.82599 (18)	0.7907 (2)	0.0690 (8)	
H5	0.335630	0.792592	0.797560	0.083*	
C6	0.1626 (3)	0.84274 (15)	0.70451 (19)	0.0571 (6)	
C7	0.2030 (3)	0.81265 (14)	0.62430 (19)	0.0529 (6)	
C8	0.0973 (3)	0.82935 (15)	0.54556 (19)	0.0571 (7)	
C9	-0.0392 (3)	0.87693 (18)	0.5469 (2)	0.0669 (8)	
H9	-0.110214	0.885782	0.493097	0.080*	
C10	0.2968 (3)	0.84632 (15)	0.41666 (17)	0.0549 (6)	
C11	0.4327 (3)	0.80964 (17)	0.3971 (2)	0.0649 (8)	
H11	0.438815	0.757924	0.399994	0.078*	
C12	0.5601 (4)	0.85057 (18)	0.3730 (2)	0.0699 (8)	
H12	0.651240	0.825780	0.359412	0.084*	
C13	0.5542 (4)	0.92746 (17)	0.3688 (2)	0.0676 (8)	
C14	0.4163 (4)	0.96262 (17)	0.3886 (2)	0.0755 (9)	
H14	0.410682	1.014372	0.386521	0.091*	
C15	0.2875 (4)	0.92320 (17)	0.4111 (2)	0.0708 (8)	
H15	0.194724	0.947991	0.422600	0.085*	
C16	0.6935 (4)	0.9711 (2)	0.3433 (3)	0.0968 (12)	
H16A	0.758596	0.992709	0.395828	0.145*	
H16B	0.650002	1.009876	0.302399	0.145*	
H16C	0.761151	0.938456	0.315502	0.145*	
C17	0.3276 (3)	0.68933 (15)	0.6411 (2)	0.0591 (7)	
H17A	0.221619	0.671292	0.610173	0.071*	

H17B	0.332639	0.682536	0.704646	0.071*	
C18	0.4648 (3)	0.64532 (16)	0.6112 (2)	0.0629 (7)	
H18A	0.452600	0.648235	0.546801	0.076*	
H18B	0.456382	0.593353	0.627312	0.076*	
C19	0.6334 (3)	0.67519 (16)	0.65413 (19)	0.0610 (7)	
H19	0.643943	0.669921	0.718917	0.073*	
C20	0.6433 (4)	0.75735 (18)	0.6337 (2)	0.0705 (8)	
H20A	0.636820	0.764020	0.570004	0.085*	
H20B	0.748421	0.776840	0.663831	0.085*	
C21	0.5054 (4)	0.80045 (17)	0.6634 (3)	0.0726 (9)	
H21A	0.517450	0.797924	0.727861	0.087*	
H21B	0.510842	0.852386	0.646572	0.087*	
C22	0.7719 (4)	0.63318 (19)	0.6266 (2)	0.0780 (10)	
O3A	0.8692 (12)	0.6593 (9)	0.5867 (10)	0.110 (4)	0.562 (12)
O4A	0.7720 (9)	0.5613 (2)	0.6503 (6)	0.083 (2)	0.562 (12)
C23A	0.8975 (13)	0.5082 (7)	0.6336 (6)	0.102 (4)	0.562 (12)
H23A	0.925138	0.473765	0.683210	0.123*	0.562 (12)
H23B	0.996805	0.534136	0.625668	0.123*	0.562 (12)
C24A	0.8233 (12)	0.4672 (7)	0.5499 (7)	0.112 (3)	0.562 (12)
H24A	0.812699	0.500471	0.499914	0.169*	0.562 (12)
H24B	0.716630	0.448644	0.555390	0.169*	0.562 (12)
H24C	0.893277	0.426205	0.541008	0.169*	0.562 (12)
O3B	0.9009 (14)	0.6554 (14)	0.6125 (15)	0.132 (7)	0.438 (12)
O4B	0.7400 (14)	0.5610 (4)	0.6108 (11)	0.135 (6)	0.438 (12)
C23B	0.888 (2)	0.5271 (7)	0.5881 (13)	0.122 (6)	0.438 (12)
H23C	0.986565	0.552319	0.618191	0.147*	0.438 (12)
H23D	0.884938	0.528434	0.524241	0.147*	0.438 (12)
C24B	0.8811 (16)	0.4482 (5)	0.6209 (14)	0.124 (6)	0.438 (12)
H24D	0.782857	0.424517	0.589912	0.187*	0.438 (12)
H24E	0.880177	0.448590	0.683798	0.187*	0.438 (12)
H24F	0.975808	0.421342	0.609985	0.187*	0.438 (12)

Atomic displacement parameters (\AA^2)

	U^{11}	U^{22}	U^{33}	U^{12}	U^{13}	U^{23}
S1	0.0576 (4)	0.0605 (5)	0.0624 (5)	-0.0034 (3)	0.0045 (3)	-0.0067 (3)
O1	0.0859 (15)	0.0524 (12)	0.0821 (16)	-0.0119 (10)	0.0206 (12)	-0.0138 (10)
O2	0.0629 (13)	0.1024 (18)	0.0651 (13)	0.0003 (11)	-0.0052 (10)	-0.0052 (12)
N1	0.0643 (15)	0.0667 (16)	0.0800 (18)	0.0106 (12)	0.0159 (13)	-0.0014 (13)
N2	0.0525 (13)	0.0452 (12)	0.0690 (15)	-0.0003 (9)	0.0105 (11)	-0.0004 (10)
C1	0.0627 (16)	0.0499 (15)	0.0722 (19)	0.0008 (12)	0.0184 (14)	-0.0022 (13)
C2	0.079 (2)	0.073 (2)	0.083 (2)	0.0051 (16)	0.0285 (18)	-0.0110 (17)
C3	0.100 (3)	0.085 (2)	0.078 (2)	-0.007 (2)	0.035 (2)	-0.0181 (19)
C4	0.106 (3)	0.075 (2)	0.063 (2)	-0.003 (2)	0.0190 (18)	-0.0012 (16)
C5	0.079 (2)	0.0652 (18)	0.0626 (19)	0.0032 (15)	0.0113 (15)	0.0011 (15)
C6	0.0622 (16)	0.0500 (15)	0.0603 (17)	-0.0040 (12)	0.0143 (12)	-0.0008 (12)
C7	0.0490 (14)	0.0428 (13)	0.0662 (17)	-0.0034 (10)	0.0088 (12)	-0.0001 (12)
C8	0.0551 (15)	0.0489 (15)	0.0658 (17)	0.0006 (11)	0.0071 (12)	-0.0013 (12)

C9	0.0555 (16)	0.0664 (19)	0.076 (2)	0.0085 (13)	0.0058 (13)	0.0055 (15)
C10	0.0566 (15)	0.0512 (15)	0.0548 (15)	0.0017 (11)	0.0049 (11)	-0.0003 (12)
C11	0.0641 (18)	0.0492 (15)	0.081 (2)	0.0081 (13)	0.0120 (15)	0.0012 (14)
C12	0.0590 (17)	0.0669 (19)	0.085 (2)	0.0080 (14)	0.0157 (15)	0.0062 (16)
C13	0.0655 (18)	0.0618 (18)	0.071 (2)	0.0006 (14)	0.0020 (14)	0.0111 (14)
C14	0.083 (2)	0.0476 (16)	0.098 (2)	0.0051 (15)	0.0211 (18)	0.0097 (15)
C15	0.0688 (19)	0.0560 (18)	0.090 (2)	0.0118 (14)	0.0196 (16)	0.0005 (15)
C16	0.077 (2)	0.090 (3)	0.122 (3)	-0.0133 (19)	0.014 (2)	0.031 (2)
C17	0.0572 (16)	0.0496 (15)	0.0722 (18)	0.0004 (12)	0.0166 (13)	0.0017 (13)
C18	0.0643 (17)	0.0509 (15)	0.0748 (19)	0.0046 (12)	0.0159 (14)	-0.0026 (14)
C19	0.0553 (15)	0.0706 (18)	0.0576 (16)	0.0056 (13)	0.0120 (12)	0.0058 (14)
C20	0.0494 (16)	0.076 (2)	0.085 (2)	-0.0058 (14)	0.0087 (15)	0.0061 (16)
C21	0.0569 (17)	0.0540 (17)	0.104 (3)	-0.0059 (13)	0.0070 (16)	-0.0066 (16)
C22	0.064 (2)	0.095 (3)	0.078 (2)	0.0186 (19)	0.0220 (17)	0.002 (2)
O3A	0.078 (5)	0.159 (8)	0.101 (5)	0.047 (5)	0.037 (4)	0.034 (5)
O4A	0.068 (3)	0.064 (3)	0.122 (7)	0.012 (2)	0.031 (3)	-0.019 (3)
C23A	0.091 (5)	0.111 (9)	0.104 (7)	0.014 (6)	0.015 (5)	-0.006 (6)
C24A	0.093 (6)	0.091 (7)	0.153 (9)	-0.007 (5)	0.021 (6)	-0.010 (7)
O3B	0.058 (5)	0.167 (11)	0.177 (17)	0.009 (6)	0.039 (8)	0.054 (10)
O4B	0.129 (9)	0.149 (9)	0.141 (12)	0.072 (7)	0.062 (8)	0.008 (6)
C23B	0.107 (9)	0.134 (12)	0.144 (14)	0.056 (9)	0.068 (10)	0.002 (11)
C24B	0.093 (8)	0.059 (6)	0.229 (19)	0.025 (5)	0.050 (10)	-0.024 (8)

Geometric parameters (Å, °)

S1—O1	1.428 (2)	C16—H16B	0.9600
S1—O2	1.438 (2)	C16—H16C	0.9600
S1—C8	1.771 (3)	C17—H17A	0.9700
S1—C10	1.755 (3)	C17—H17B	0.9700
N1—C1	1.366 (4)	C17—C18	1.518 (4)
N1—C9	1.306 (4)	C18—H18A	0.9700
N2—C7	1.419 (3)	C18—H18B	0.9700
N2—C17	1.469 (3)	C18—C19	1.523 (4)
N2—C21	1.476 (3)	C19—H19	0.9800
C1—C2	1.407 (4)	C19—C20	1.512 (4)
C1—C6	1.412 (4)	C19—C22	1.494 (3)
C2—H2	0.9300	C20—H20A	0.9700
C2—C3	1.367 (5)	C20—H20B	0.9700
C3—H3	0.9300	C20—C21	1.514 (4)
C3—C4	1.384 (5)	C21—H21A	0.9700
C4—H4	0.9300	C21—H21B	0.9700
C4—C5	1.364 (4)	C22—O3A	1.191 (5)
C5—H5	0.9300	C22—O4A	1.340 (4)
C5—C6	1.405 (4)	C22—O3B	1.194 (5)
C6—C7	1.431 (4)	C22—O4B	1.334 (5)
C7—C8	1.381 (4)	O4A—C23A	1.464 (5)
C8—C9	1.417 (4)	C23A—H23A	0.9700
C9—H9	0.9300	C23A—H23B	0.9700

C10—C11	1.381 (4)	C23A—C24A	1.502 (5)
C10—C15	1.383 (4)	C24A—H24A	0.9600
C11—H11	0.9300	C24A—H24B	0.9600
C11—C12	1.387 (4)	C24A—H24C	0.9600
C12—H12	0.9300	O4B—C23B	1.462 (5)
C12—C13	1.382 (4)	C23B—H23C	0.9700
C13—C14	1.383 (4)	C23B—H23D	0.9700
C13—C16	1.501 (4)	C23B—C24B	1.506 (5)
C14—H14	0.9300	C24B—H24D	0.9600
C14—C15	1.373 (4)	C24B—H24E	0.9600
C15—H15	0.9300	C24B—H24F	0.9600
C16—H16A	0.9600		
O1—S1—O2	117.38 (14)	N2—C17—H17B	109.7
O1—S1—C8	111.76 (13)	N2—C17—C18	109.8 (2)
O1—S1—C10	109.63 (13)	H17A—C17—H17B	108.2
O2—S1—C8	104.97 (13)	C18—C17—H17A	109.7
O2—S1—C10	106.93 (13)	C18—C17—H17B	109.7
C10—S1—C8	105.39 (13)	C17—C18—H18A	109.4
C9—N1—C1	116.9 (3)	C17—C18—H18B	109.4
C7—N2—C17	114.9 (2)	C17—C18—C19	111.2 (2)
C7—N2—C21	117.0 (2)	H18A—C18—H18B	108.0
C17—N2—C21	113.5 (2)	C19—C18—H18A	109.4
N1—C1—C2	116.7 (3)	C19—C18—H18B	109.4
N1—C1—C6	123.1 (3)	C18—C19—H19	107.7
C2—C1—C6	120.1 (3)	C20—C19—C18	109.5 (2)
C1—C2—H2	119.8	C20—C19—H19	107.7
C3—C2—C1	120.4 (3)	C22—C19—C18	112.9 (3)
C3—C2—H2	119.8	C22—C19—H19	107.7
C2—C3—H3	120.1	C22—C19—C20	111.1 (2)
C2—C3—C4	119.8 (3)	C19—C20—H20A	109.4
C4—C3—H3	120.1	C19—C20—H20B	109.4
C3—C4—H4	119.5	C19—C20—C21	111.3 (2)
C5—C4—C3	120.9 (3)	H20A—C20—H20B	108.0
C5—C4—H4	119.5	C21—C20—H20A	109.4
C4—C5—H5	119.3	C21—C20—H20B	109.4
C4—C5—C6	121.4 (3)	N2—C21—C20	109.8 (2)
C6—C5—H5	119.3	N2—C21—H21A	109.7
C1—C6—C7	118.5 (3)	N2—C21—H21B	109.7
C5—C6—C1	117.3 (3)	C20—C21—H21A	109.7
C5—C6—C7	124.2 (3)	C20—C21—H21B	109.7
N2—C7—C6	124.0 (2)	H21A—C21—H21B	108.2
C8—C7—N2	119.2 (2)	O3A—C22—C19	124.7 (8)
C8—C7—C6	116.8 (2)	O3A—C22—O4A	123.3 (9)
C7—C8—S1	123.0 (2)	O4A—C22—C19	111.9 (4)
C7—C8—C9	119.7 (3)	O3B—C22—C19	129.6 (13)
C9—C8—S1	117.3 (2)	O3B—C22—O4B	116.4 (14)
N1—C9—C8	124.6 (3)	O4B—C22—C19	113.9 (5)

N1—C9—H9	117.7	C22—O4A—C23A	123.1 (7)
C8—C9—H9	117.7	O4A—C23A—H23A	110.5
C11—C10—S1	120.9 (2)	O4A—C23A—H23B	110.5
C11—C10—C15	120.0 (3)	O4A—C23A—C24A	106.0 (8)
C15—C10—S1	118.9 (2)	H23A—C23A—H23B	108.7
C10—C11—H11	120.3	C24A—C23A—H23A	110.5
C10—C11—C12	119.5 (3)	C24A—C23A—H23B	110.5
C12—C11—H11	120.3	C23A—C24A—H24A	109.5
C11—C12—H12	119.4	C23A—C24A—H24B	109.5
C13—C12—C11	121.3 (3)	C23A—C24A—H24C	109.5
C13—C12—H12	119.4	H24A—C24A—H24B	109.5
C12—C13—C14	118.0 (3)	H24A—C24A—H24C	109.5
C12—C13—C16	120.7 (3)	H24B—C24A—H24C	109.5
C14—C13—C16	121.4 (3)	C22—O4B—C23B	107.5 (9)
C13—C14—H14	119.1	O4B—C23B—H23C	111.1
C15—C14—C13	121.8 (3)	O4B—C23B—H23D	111.1
C15—C14—H14	119.1	O4B—C23B—C24B	103.2 (8)
C10—C15—H15	120.3	H23C—C23B—H23D	109.1
C14—C15—C10	119.4 (3)	C24B—C23B—H23C	111.1
C14—C15—H15	120.3	C24B—C23B—H23D	111.1
C13—C16—H16A	109.5	C23B—C24B—H24D	109.5
C13—C16—H16B	109.5	C23B—C24B—H24E	109.5
C13—C16—H16C	109.5	C23B—C24B—H24F	109.5
H16A—C16—H16B	109.5	H24D—C24B—H24E	109.5
H16A—C16—H16C	109.5	H24D—C24B—H24F	109.5
H16B—C16—H16C	109.5	H24E—C24B—H24F	109.5
N2—C17—H17A	109.7		
S1—C8—C9—N1	-175.8 (2)	C9—N1—C1—C2	-179.0 (3)
S1—C10—C11—C12	175.7 (2)	C9—N1—C1—C6	0.5 (4)
S1—C10—C15—C14	-176.9 (3)	C10—S1—C8—C7	-71.5 (3)
O1—S1—C8—C7	47.6 (3)	C10—S1—C8—C9	106.4 (2)
O1—S1—C8—C9	-134.6 (2)	C10—C11—C12—C13	0.5 (5)
O1—S1—C10—C11	4.5 (3)	C11—C10—C15—C14	-1.9 (5)
O1—S1—C10—C15	179.5 (2)	C11—C12—C13—C14	-0.6 (5)
O2—S1—C8—C7	175.8 (2)	C11—C12—C13—C16	179.5 (3)
O2—S1—C8—C9	-6.4 (3)	C12—C13—C14—C15	-0.5 (5)
O2—S1—C10—C11	-123.7 (2)	C13—C14—C15—C10	1.7 (5)
O2—S1—C10—C15	51.3 (3)	C15—C10—C11—C12	0.8 (4)
N1—C1—C2—C3	176.8 (3)	C16—C13—C14—C15	179.4 (3)
N1—C1—C6—C5	-175.5 (3)	C17—N2—C7—C6	83.1 (3)
N1—C1—C6—C7	4.2 (4)	C17—N2—C7—C8	-98.2 (3)
N2—C7—C8—S1	1.7 (4)	C17—N2—C21—C20	57.5 (3)
N2—C7—C8—C9	-176.1 (2)	C17—C18—C19—C20	-55.7 (3)
N2—C17—C18—C19	55.9 (3)	C17—C18—C19—C22	179.8 (2)
C1—N1—C9—C8	-3.7 (5)	C18—C19—C20—C21	55.9 (3)
C1—C2—C3—C4	-1.0 (5)	C18—C19—C22—O3A	117.3 (10)
C1—C6—C7—N2	173.2 (2)	C18—C19—C22—O4A	-61.1 (6)

C1—C6—C7—C8	-5.5 (4)	C18—C19—C22—O3B	143.1 (14)
C2—C1—C6—C5	3.9 (4)	C18—C19—C22—O4B	-32.5 (9)
C2—C1—C6—C7	-176.4 (3)	C19—C20—C21—N2	-56.2 (4)
C2—C3—C4—C5	3.3 (5)	C19—C22—O4A—C23A	-178.2 (7)
C3—C4—C5—C6	-1.9 (5)	C19—C22—O4B—C23B	-177.9 (9)
C4—C5—C6—C1	-1.7 (5)	C20—C19—C22—O3A	-6.2 (11)
C4—C5—C6—C7	178.7 (3)	C20—C19—C22—O4A	175.4 (5)
C5—C6—C7—N2	-7.1 (4)	C20—C19—C22—O3B	19.6 (15)
C5—C6—C7—C8	174.1 (3)	C20—C19—C22—O4B	-156.0 (9)
C6—C1—C2—C3	-2.6 (5)	C21—N2—C7—C6	-53.7 (4)
C6—C7—C8—S1	-179.56 (19)	C21—N2—C7—C8	124.9 (3)
C6—C7—C8—C9	2.7 (4)	C21—N2—C17—C18	-57.4 (3)
C7—N2—C17—C18	164.2 (2)	C22—C19—C20—C21	-178.7 (3)
C7—N2—C21—C20	-165.0 (2)	C22—O4A—C23A—C24A	-98.1 (14)
C7—C8—C9—N1	2.1 (5)	C22—O4B—C23B—C24B	150 (2)
C8—S1—C10—C11	124.9 (2)	O3A—C22—O4A—C23A	3.4 (14)
C8—S1—C10—C15	-60.1 (3)	O3B—C22—O4B—C23B	5.9 (17)

Hydrogen-bond geometry (Å, °)

<i>D</i> —H... <i>A</i>	<i>D</i> —H	H... <i>A</i>	<i>D</i> ... <i>A</i>	<i>D</i> —H... <i>A</i>
C4—H4...O3A ⁱ	0.93	2.52	3.421 (16)	163
C5—H5...O2 ⁱⁱ	0.93	2.58	3.415 (4)	149

Symmetry codes: (i) $x-1/2, -y+3/2, z+1/2$; (ii) $x+1/2, -y+3/2, z+1/2$.